

Gaussian beam effects on the photon correlation spectrum from a flowing Brownian motion system

Thomas W. Taylor and Christopher M. Sorensen

The theory of photon correlation spectroscopy for a flowing system of diffusing particles was extended to include the Gaussian shape properties of an incident light beam. We found that the characteristic time of the coherent translational term caused by the bulk flow of the system was independent of the distance between the scattering volume and the focal point of the incident beam. The flow velocity and beam radius at the focus determined the characteristic time of this term. We also studied the effect of defocusing on the amplitude of the incoherent or number density term of the homodyne-detected intensity autocorrelation function. We verified our results experimentally using a flowing dioctylphthalate aerosol.

I. Introduction

Photon correlation spectroscopy (PCS) has proved useful in the study of diffusional processes as well as particle sizing in various systems. A number of practical applications of recent interest involved flowing systems of aerosols¹ or diffusing soot particles in flames.²⁻⁴ Chowdhury *et al.*,⁵ following the work of Edwards *et al.*,⁶ have discussed the theory of PCS for a flowing system of Brownian particles. They assumed a spherically symmetric Gaussian incident beam with a plane wave front in the scattering volume and found the homodyne autocorrelation function to be

$$I_2(t) = \langle N \rangle^2 [1 + \exp(-2Dq^2t) \exp(-v^2t^2/w^2) + 2^{-3/2} \langle N \rangle^{-1} \exp(-v^2t^2/w^2)]. \quad (1)$$

Here $\langle N \rangle$ is the average number of particles in the scattering volume, D is the particle diffusion constant, v is the flow velocity, w is the beam radius, and \mathbf{q} is the scattering wave vector with magnitude $q = 4\pi n/\lambda \sin\theta/2$, where λ , n , and θ are the wavelength, medium refractive index, and scattering angle, respectively.

In this result, the diffusional term with characteristic time $\tau_1 = (2Dq^2)^{-1}$ is multiplied by a Gaussian-in-time translational term with characteristic time $\tau_2 = w/v$. For high flow rate, narrow beam radius, or both, τ_2 may be $< \tau_1$. If so, the size information in τ_1 will become difficult to extract because the τ_2 term will dominate the decay. Apparently one way to alleviate this problem is to increase w by defocusing the incident beam. In this paper, we will show that this remedy will not work, because the second term in Eq. (1) should be

modified by replacing w with w_1 , the beam radius at the focus of the incident Gaussian beam.

In Sec. II we extend the procedure of Chowdhury *et al.*⁵ to include the more general spherical wave front of a Gaussian incident beam. This will allow us to examine the effects of moving the scattering volume away from the focal point of the incident beam where the wave front is plane. In Sec. III we describe an experiment on a flowing dioctylphthalate aerosol to verify the theoretical results. Section IV details the data analysis techniques, and Sec. V compares the experimental results to the theoretical predictions.

II. Theory

In this section we briefly review the properties of a propagating focused Gaussian-profile beam. A full description of these properties may be found in Kogelnik.⁷ We then apply this more general description of the incident beam to the procedure presented by Chowdhury *et al.*⁵ and arrive at a theoretical description of both the heterodyned and homodyned scattered light intensity autocorrelation function.

A laser beam operating in the TEM₀₀ mode may be described as a Gaussian beam with a spherical wave front. The amplitude profile for a beam propagating in the positive z direction (Fig. 1) can be written as

$$P(r_{xy}) = E_0 \exp(-r_{xy}^2/w^2 - ikr_{xy}^2/2R), \quad (2a)$$

where the principal parameters describing the wave are w , the beam radius, and R , the radius of curvature of the wave front. Also in Eq. (2), \mathbf{k} is the propagation vector with magnitude $k = 2\pi n/\lambda$, and $i = \sqrt{-1}$. Finally, r_{xy} is the perpendicular distance from the optical axis of the beam.

We will approximate the cylindrically symmetric beam profile in Eq. (2a) by a more spherically symmetric form:

The authors are with Kansas State University, Physics Department, Manhattan, Kansas 66506.

Received 15 January 1986.

0003-6935/86/142421-06\$02.00/0.

© 1986 Optical Society of America.

$$P(\mathbf{r}) = E_0 \exp(-r^2/w^2 - ikr_{xy}^2/2R). \quad (2b)$$

This is not unreasonable because the view of the incident Gaussian beam will most likely be vignetted somewhat on its way to the detector. We note that $r^2 = x^2 + y^2 + z^2$, while $r_{xy}^2 = x^2 + y^2$.

Figure 1 shows a Gaussian beam incident on a thin lens of focal length f . The focused beam radius w_1 is related to the incident beam radius w_0 , where the wave front was last plane before passing through the lens by the expression

$$\frac{1}{w_1^2} = (1 - z_0/f)^2 + (\pi w_0/\lambda f)^2. \quad (3)$$

Here z_0 is the distance from the focusing lens to the point where the incident wave front was last plane.

The location z_1 of the focal point where the phase front is again plane after passing through the lens is given by

$$(z_1 - f) = (z_0 - f) \frac{f^2}{(z_0 - f)^2 + (\pi w_0^2/\lambda)^2}. \quad (4)$$

The beam radius w , a distance z from this focal point, is

$$w^2 = w_1^2 [1 + (\lambda z/\pi w_1^2)^2], \quad (5)$$

and the radius of curvature of the wave front is

$$R = z[1 + (\pi w_1^2/\lambda z)^2]. \quad (6)$$

We may use Eqs. (5) and (6) to find the ratio of the beam radius to the radius of curvature of the wave front to be

$$\frac{w}{R} = \frac{\lambda}{\pi w_1} [1 + (\pi w_1^2/\lambda z)^2]^{-1/2}. \quad (7)$$

With these relationships, we are now ready to examine the effects of scattering from a Gaussian beam at any position z along the beam. We will consider light scattered in the y - z plane (horizontal) with incident polarization in the x direction (vertical). In this case the scattered electric field will have a vertical polarization with magnitude

$$E_s(t) = \sum_{j=1}^N \exp(i\mathbf{q} \cdot \mathbf{r}_j) P(\mathbf{r}_j), \quad (8)$$

where the sum is over all N particles in the system, \mathbf{q} is the scattering wave vector, and \mathbf{r}_j is the position vector

of the j th particle. $P(\mathbf{r})$ is the amplitude profile given by Eq. (2b).

It is convenient in a flowing system undergoing Brownian diffusion to decompose the position vector \mathbf{r}_j into a translational (bulk flow) term and a diffusional (Brownian motion) term,⁶

$$\mathbf{r}_j(t) = \mathbf{v}t + \mathbf{r}'_j(t). \quad (9)$$

Here $\mathbf{r}'_j(t)$ is due only to the diffusional motion, and \mathbf{v} is the bulk flow velocity assumed to be in the x direction.

To determine the heterodyne- or homodyne-detected autocorrelation functions, we first obtain the two autocorrelation functions defined by⁸

$$I_1(t) = \langle E_s(t) E_s^*(0) \rangle, \quad (10)$$

$$I_2(t) = \langle |E_s(t)|^2 |E_s(0)|^2 \rangle, \quad (11)$$

where the brackets indicate an ensemble average. I_1 is needed to determine the heterodyne-detected autocorrelation function, and I_2 is needed for the homodyne-detected autocorrelation function. The relationship between these intensity correlation functions and the detected functions can be found in Berne and Pecora.⁸

We must recognize that the averages implied by the brackets in both Eqs. (10) and (11) are in fact composed of two distinct ensemble averages. One is over the diffusional motion, which will be denoted by $\langle \dots \rangle_{\delta \mathbf{r}}$, and the other is over the translational motion, which will be denoted by $\langle \dots \rangle_{\mathbf{r}}$. For simplicity we will limit the displacement due to the diffusion to be much less than the beam radius w over a time comparable with the experimental correlation time τ_1 . This means the two ensemble averages defined above are independent and separable.

We use Eqs. (8), (9), and (10) to write the field autocorrelation function as

$$I_1(t) = \exp(i\mathbf{q} \cdot \mathbf{v}t) \sum_{j,k} \langle \exp[i\mathbf{q} \cdot \delta \mathbf{r}_{jk}(t)] \rangle_{\delta \mathbf{r}} \times \langle P[\mathbf{r}_j(t)] P^*[\mathbf{r}_k(0)] \rangle_{\mathbf{r}}, \quad (12)$$

where $\delta \mathbf{r}_{jk} = \mathbf{r}'_j(t) - \mathbf{r}'_k(0)$. If the particles are independent, i.e., noninteracting, only the $j = k$ terms survive. The well-known diffusional average is

$$\langle \exp(i\mathbf{q} \cdot \delta \mathbf{r}(t)) \rangle_{\delta \mathbf{r}} = \exp(-Dq^2t). \quad (13)$$

To effectively change the phase in Eq. (13), $\delta \mathbf{r} \sim q^{-1}$. Since typically $q^{-1} < 1 \mu\text{m}$, $\delta \mathbf{r}$ is small compared with the beam waist w . For this situation, the translational average is an average over the probability of finding a particle initially in a volume element. This probability is $V_T^{-1} d^3r$, where V_T is the total volume of the system. The translational average is written as

$$\begin{aligned} & E_0^2/V_T \int d^3r \exp[-(\mathbf{r} + \mathbf{v}t)^2/w^2 - ikr_{xy}^2/2R] \\ & \times \exp[-r^2/w^2 + ikr_{xy}^2/2R] \\ & = \frac{E_0^2 V_s}{V_T} \exp \left[-\frac{v^2 t^2}{2w^2} (1 + k^2 w^4/4R^2) \right], \end{aligned} \quad (14)$$

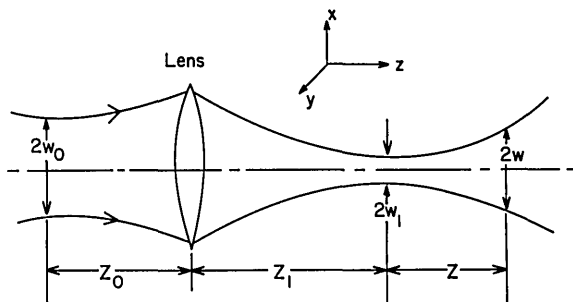


Fig. 1. Propagation of a Gaussian beam through a lens. Definition of beam radii and distances.

where $V_s = (\pi/2)^{3/2} w^3$ is an effective scattering volume found by integrating the intensity function, $P^*(\mathbf{r})P(\mathbf{r})$, over all space. Finally, summing over all the particles N , the field autocorrelation function is

$$I_1 = I_0 \langle N \rangle \exp(i\mathbf{q} \cdot \mathbf{v}t) \exp(-Dq^2t) \exp\left[\frac{-v^2t^2}{2w^2} (1 + k^2w^4/4R^2)\right]. \quad (15)$$

Here $\langle N \rangle = NV_s/V_T$ is the average number of particles in the scattering volume.

Equation (15) is the product of three terms, a sinusoidal Doppler shift term due to the translational motion, an exponential decay due to the diffusional motion, and a modified Gaussian-in-time term caused by the translational motion of the particles through the scattering volume.

This last term merits further attention. We can rewrite it as

$$\exp(-v^2t^2/2w^2) \exp(-v^2t^2k^2w^2/8R^2). \quad (16)$$

At the focal point of the lens, $R = \infty$, and the result of Chowdhury *et al.*⁵ is obtained. We now use Eq. (7) for the ratio w/R to rewrite Eq. (16) as

$$\exp(-v^2t^2/2w^2) \exp\left\{-\frac{v^2t^2}{2w_1^2} [1 + (\pi w_1^2/\lambda z)^2]^{-1}\right\} = \exp(-v^2t^2/2w'^2), \quad (17)$$

where

$$\frac{1}{w'^2} = \frac{1}{w^2} + \frac{1}{w_1^2 [1 + (\pi w_1^2/\lambda z)^2]}. \quad (18)$$

Here w' is a modified beam radius corresponding to a combination in Eq. (18) of the true beam radius w and a term caused by the distribution of incident propagation wave vectors due to the spherical wave front. If, however, we now use Eqs. (5) and (8), we find

$$w' = w_1, \quad (19)$$

where w_1 is the beam radius at the focus. Therefore, I_1 has the form

$$I_1 = I_0 \langle N \rangle \exp(i\mathbf{q} \cdot \mathbf{v}t) \exp(-Dq^2t) \exp(-v^2t^2/2w_1^2). \quad (20)$$

This is the same as that given by Chowdhury *et al.*⁵ except that the beam radius w at any arbitrary position z of the scattering volume is replaced by w_1 , the beam radius at the focus. Thus the beam-transit or Gaussian-in-time term is independent of the position of the scattering volume relative to the focal point of the incident beam.

The result in Eq. (20) is somewhat surprising. Heretofore workers had taken the Gaussian-in-time term to be a beam transit term dependent on the width w of the beam at the scattering volume. Equations (16)–(20) show that this is not the case but is instead a combination of the width of the beam and the spread in incident wave vectors as represented by the curvature of the spherical wave front. It is this combination that is represented by w_1 , the focused beam radius, and is a unique function of w_0 , f , and z_0 . Edwards *et al.*,⁶ while they did not present an explicit derivation, alluded to the interrelationship between the beam transit time

and the spread in incident wave vectors. Also, Estes *et al.*⁹ showed the independence on focal position of the spectral width of light scattered from a rotating ground glass.

For application of PCS to sizing of a flowing particulate system, the Gaussian-in-time term should decay much slower than the diffusional term which contains the size information. Equation (20) shows this cannot be achieved by defocusing, i.e., changing z . Rather w_0 , z_0 , or f must be changed.

The calculation of I_2 is somewhat cumbersome so we will concentrate only on the translational averages as the diffusional averages are the same as those found in Chowdhury *et al.*⁵ Using Eqs. (8), (9), and (11) and the condition $\delta r(t) \ll vt$ as before, the translational average is

$$\left\langle \sum_{jklm} P[\mathbf{r}_j(t)] P^*[\mathbf{r}_k(t)] P[\mathbf{r}_l(o)] P^*[\mathbf{r}_m(o)] \right\rangle. \quad (21)$$

Particle independence requires that the ensemble average vanish if any of the particle indices are distinct. Thus only two kinds of term survive, those with $j = k$ and $l = m$ including $j = k = l = m$ and those with $j = m$ and $k = l$, $j \neq k$.

With $j = k$ and $l = m$, $j \neq l$, and Eq. (2), Eq. (21) becomes

$$\frac{I_0^2}{V_T^2} \sum_{j \neq l}^N \int d^3r_j \exp[-2(\mathbf{r}_j + \mathbf{v}t)^2/w^2] \int d^3r_l \exp(-2r_l^2/w^2) = I_0^2 \sum_{j \neq l} (V_s/V_T)^2. \quad (22)$$

Summing over j and l yields

$$I_0^2 \sum (V_s/V_T)^2 = I_0^2 \langle N_s(N_s - 1) \rangle, \quad (23)$$

where N_s is the number of particles in the scattering volume. N_s should follow the Poisson distribution so that $\langle N_s(N_s - 1) \rangle = \langle N \rangle^2$, where $\langle N \rangle$ is the average number of particles in the scattering volume.⁸

When $j = k = l = m$, Eq. (21) becomes

$$\begin{aligned} I_0^2/V_T \sum_j^N \int d^3r_j \exp[-2(\mathbf{r}_j + \mathbf{v}t)^2/w^2] \exp(-2r_j^2/w^2) \\ = I_0^2 \langle N \rangle 2^{-3/2} \exp(-v^2t^2/w^2). \end{aligned} \quad (24)$$

When $j = m$, $k = l$, and $j \neq k$ Eq. (21) becomes

$$\sum_{j \neq l} \langle P[\mathbf{r}_j(t)] P^*[\mathbf{r}_j(o)] \rangle_{r_j} \langle P^*[\mathbf{r}_l(t)] P[\mathbf{r}_l(o)] \rangle_{r_l}, \quad (25)$$

where we have used particle independence to separate the ensemble averages. The symmetry of the amplitude function causes the second average in the product to be identical to the first average. Thus

$$\sum_{j \neq l} \langle P[\mathbf{r}_j(t)] P^*[\mathbf{r}_j(o)] \rangle_{r_j}^2 = \sum_{j \neq l} I_0^2 \frac{V_s^2}{V_T^2} \exp(-v^2t^2/w_1^2), \quad (26)$$

where we have made use of Eqs. (14), (16), (17), and (19). Summing over j and using the properties of the Poisson distribution, Eq. (26) becomes

$$I_0^2 \langle N \rangle^2 \exp(-v^2 t^2 / w_1^2). \quad (27)$$

Chowdhury *et al.*⁵ found the diffusional average to be of no consequence (i.e., equal to unity) for the $j = k$ and $l = m$ including the $j = k = l = m$ term and $\langle \dots \rangle_{\delta r} = \exp(-2Dq^2 t)$ for the $j = m, k = l$, and $j \neq k$ term. Combining these results with Eqs. (23), (24), and (27) we can write the homodyne intensity autocorrelation function as

$$I_2(t) = \langle N \rangle^2 [1 + \exp(-2Dq^2 t) \exp(-v^2 t^2 / w_1^2) + 2^{-3/2} \langle N \rangle^{-1} \exp(-v^2 t^2 / w^2)]. \quad (28)$$

The second term in Eq. (28) again shows the competition between the diffusional and translational motions that was seen in I_1 . The translational term is dependent on the focused beam radius and is independent of the location of V_s . The last term, sometimes referred to as the incoherent or number density term, is dependent on the number of particles in the scattering volume as well as the beam radius at V_s . Thus this term can be made longer in time and reduced in relative importance by moving away from the focal point of the lens. By increasing z , the distance between the focal point and V_s , w is increased, causing an increase in V_s and $\langle N \rangle$. The increase in w causes the Gaussian-in-time term to decay slower, and the increase in $\langle N \rangle$ causes a decrease in its relative amplitude. For scattering volumes such that w remains approximately constant across V_s ,

$$V_s \propto w^2 = w_1^2 \left[1 + \left(\frac{\lambda z}{\pi w_1^2} \right)^2 \right]. \quad (29)$$

Using the definition $\langle N \rangle = (NV_s/V_T)$ and Eq. (29) we find for $z > \pi w_1^2 / \lambda$,

$$\langle N \rangle \propto z^2. \quad (30)$$

Thus the amplitude of the incoherent term is inversely proportional to z^2 , and an increase in z greatly reduces the amplitude of the incoherent term.

III. Experiment

To verify the results of the preceding calculations of the effects of the location of the scattering volume relative to the focal point, we need to measure both the coherent and incoherent translational terms. This was accomplished by varying the diameter of the aerosol droplets and the position of the scattering volume so that the diffusional term and the two translational terms changed in relative importance.

A flowing aerosol was made using a commercial aerosol generator. The aerosol was generated by dispersing a solution of ethanol-dioctylphthalate (DOP) through a nebulizer. The resulting fog of droplets was then evaporated and recondensed to form a fairly monodisperse aerosol. The final size of the aerosol droplet was dependent on the concentration of the original ethanol DOP solution. The aerosol then flowed downward through 3.8-cm diam, 5-m long vertical glass tube. The scattered light was detected 10 cm above the bottom of the tube to ensure a stable uniform flow.

The light scattering apparatus consisted of an ar-

gon-ion laser operating in the TEM₀₀ mode at $\lambda = 5145$ Å. The beam, with polarization perpendicular to the horizontal scattering plane, passed through a lens toward the center of the flow tube. Light scattered at a 45° angle was collected by a lens and imaged onto an adjustable slit to provide suitable coherence on the photocathode of a FW 130 photomultiplier tube. The output of the PMT was amplified, discriminated, and passed to a commercial correlator where the homodyne-detected correlation function was calculated. The function was passed to a microcomputer for analysis.

To study the effect on the optics on the coherent translational term, we generated an aerosol from a 50% DOP in ethanol solution. This produced aerosol droplets 900 nm in diameter. This size was chosen to lengthen the decay time of the diffusional term to allow accurate measurement of the coherent translational term.

To study the incoherent translational term, a solution of 0.1% DOP in ethanol was used to generate an aerosol with 90-nm diam droplets. The small particle size caused the diffusional term to decay to zero rapidly allowing us to measure the incoherent term. In each case the incident beam was focused with either a 30- or 54.6-cm focal length lens and the homodyne detected correlation function measured at various values of z .

IV. Data Analysis

In the dilute limit, the homodyne-detected autocorrelation function for a flowing Brownian particle system can be written

$$C(t) = B + C \exp\left(\frac{-n\Delta t}{\tau_1}\right) \exp\left(\frac{-n^2 \Delta t^2}{\tau_2^2}\right) + A \exp\left(-\frac{n^2 \Delta t^2}{\tau_3^2}\right). \quad (31)$$

Here B is an experimental background term, C is dependent on the coherence on the photocathode, and A is dependent on $\langle N \rangle$. Time is computed as $n\Delta t$, where Δt is the correlator sample time and n is a non-negative integer. The characteristic time $\tau_1 = (2Dq^2)^{-1}$ is the diffusional correlation time, $\tau_2 = w_1/v$ corresponds to the coherent translational correlation time, and $\tau_3 = w/v$ corresponds to the incoherent translational correlation time.

Analysis of the coherent translational term was done using the method outlined in Chowdhury *et al.*⁵ In this method the function

$$Y(n\Delta t) = -\frac{1}{n\Delta t} \ln \left[\frac{C(t) - B}{C} \right] \quad (32)$$

was fit using a linear least-squares routine to

$$Y(n\Delta t) = 1/\tau_1 + \frac{1}{\tau_2^2} n\Delta t. \quad (33)$$

The use of large particles kept τ_1 large to reduce the error in τ_2 , and the background B could be varied to correct for the incoherent term.

Analysis of the correlation function to determine τ_3 and A was carried out by fitting the data to the form

$$C(t) = B + A \exp(-n^2 \Delta t^2 / \tau_3^2). \quad (34)$$

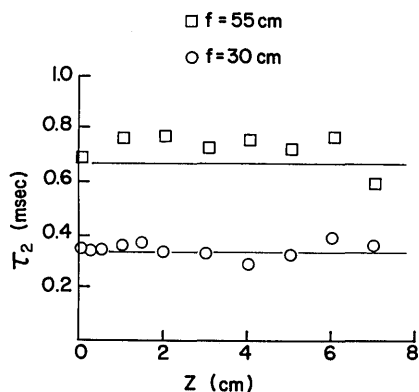


Fig. 2. Characteristic time τ_2 vs z , the distance between the scattering volume and the focal point of the incident beam, for light focused by two different lenses. The solid lines are theoretical predictions.

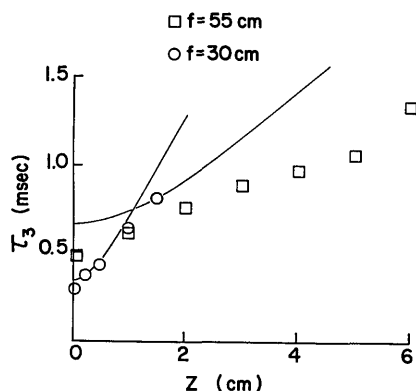


Fig. 3. Characteristic time τ_3 vs z , the distance between the scattering volume and the focal point of the incident beam, for light focused by two different lenses. The solid lines are theoretical predictions.

The coherent terms could be neglected because the small size of the droplets caused the diffusional term to decay rapidly to zero relative to the incoherent translational term. To reduce further the effects of the diffusional term, the first few data points in the correlation function were excluded from the nonlinear least-squares fitting routine. We used the Marquardt algorithm with B , A , and τ_3 as fitting parameters.

V. Experimental Results

In Sec. II we found that $\tau_2 = w_1/v$ was independent of z , the distance between the focal point and the scattering volume. A comparison of the measured and predicted values of τ_2 is shown in Fig. 2. The predicted value was determined using v , measured by a standard gas flowmeter, and w_1 , calculated using Eq. (3), and the measured value of w_0 at the output end of the laser. The experimental results show no dependence on z , verifying that τ_2 is dependent only on the focused beam waist. To emphasize the constancy of τ_2 , compare τ_2 to $\tau_3 = w/v$ in Fig. 3. $\tau_2 = \tau_3$ at $z = 0$, but τ_3 rapidly increases with z while τ_2 remains constant. The magnitudes of τ_2 are not in total agreement with $\tau_2 = w_1/v$, however. This is due to the polydispersity of the

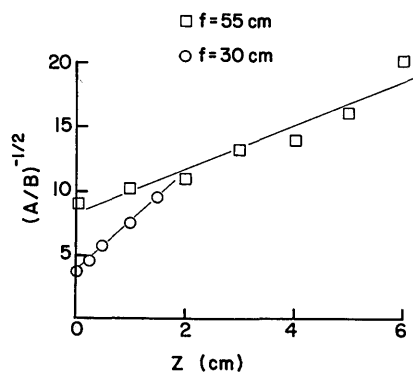


Fig. 4. Inverse square root of the amplitude of the incoherent term relative to the background $(A/B)^{-1/2}$ vs z , the distance between the scattering volume and focal point of the incident beam, for light focused by two different lenses. The solid lines are least-squares fits to the data.

aerosol droplets. Polydispersity would cause an increase in τ_2 . Thus the measured values should be somewhat larger than the predicted values, which is what we found.

The measured values of $\tau_3 = w/v$ are compared with the expected values in Fig. 3. The solid lines are found using Eqs. (3)–(5) and measured values of v , w_0 , z_0 , and z . Good agreement is seen for the 30-cm lens. The data for the 54.6 lens show the same basic shape as the expected curve, but there is considerable deviation caused by the difficulty in determining τ_3 when much of the data is buried in the noise due to the small values of A .

In Fig. 4 the measured values of $A^{-1/2}$ relative to the background B are plotted as a function of z . A linear relationship is found, as expected, from Eqs. (30) and (31). The solid lines are least-squares fits to the data. The quality of the measured data is somewhat surprising as the amplitudes varied from 1 to 6% above the background for the 30-cm lens and only 0.1–1% for the 54.6-cm lens.

VI. Conclusion

In this study we found that τ_2 , the characteristic time of the coherent translational term, is independent of the incident beam radius at the scattering volume but depends on the beam radius at the focus where the incident beam's wave front was last plane. This was a result of inclusion of the proper phase term in the equation for the incident beam, Eq. (2a) or (2b). Equations (20) and (28) represent the properly formulated heterodyne or homodyne scattered light correlation functions for flowing Brownian motion systems. Our theoretical results were verified with experiment.

We thank B. J. Olivier and J. F. Merklin for useful discussions. This work was supported by NSF grant CPE 8218415.

References

1. W. Hinds and P. C. Reist, "Aerosol Measurement by Laser Doppler Spectroscopy-I. Theory and Experimental Result for Homogeneous Aerosols," *Aerosol Sci.* **3**, 501 (1972).
2. G. B. King, C. M. Sorensen, T. W. Lester, and J. F. Merklin, "Photon Correlation Spectroscopy Used as a Particle Size Diagnostic in Sooting Flames," *Appl. Opt.* **21**, 976 (1982).
3. W. L. Flower, "Optical Measurements of Soot Formation in Premixed Flames," *Combust. Sci. Technol.* **33**, 17 (1983).
4. S. M. Scrivner, T. W. Taylor, C. M. Sorensen, and J. F. Merklin, "Soot Particle Size Distribution Measurements in a Premixed Flame Using Photon Correlation Spectroscopy," *Appl. Opt.* **25**, 291 (1986).
5. D. P. Chowdhury, C. M. Sorensen, T. W. Taylor, J. F. Merklin, and T. W. Lester, "Application of Photon Correlation Spectroscopy to Flowing Brownian Motion Systems," *Appl. Opt.* **23**, 4149 (1984).
6. R. V. Edwards, J. C. Angus, M. J. French, and J. W. Dunning, Jr., "Spectral Analysis of the Signal from the Laser Doppler Flowmeter: Time-Independent Systems," *J. Appl. Phys.* **42**, 837 (1972).
7. H. Kogelnik, "Imaging of Optical Modes—Resonators with Internal Lenses," *Bell Syst. Tech. J.* **44**, 485 (1965).
8. B. J. Berne and R. Pecora, *Dynamic Light Scattering* (Wiley, New York, 1976).
9. L. E. Estes, L. M. Narducci, and R. A. Tuft, "Scattering of Light from a Rotating Ground Glass," *J. Opt. Soc. Am.* **61**, 1301 (1971).



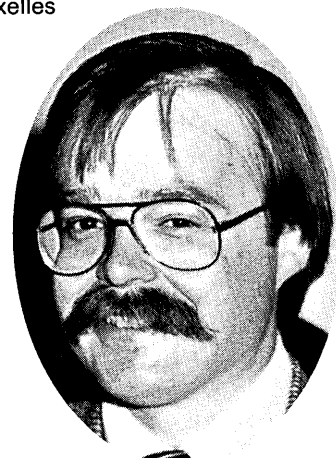
Paul Mandel
U. Libre de Bruxelles



Michael Rankin
Naval Air Development Center



Rasheed M. A. Azzam
U. New Orleans



Patrick Cheatham
Pacific Sierra Research Corp.



George Dubé
General Electric



Simon George
California State U.

photos:
F. S. Harris, Jr.